PAPER • OPEN ACCESS

Superposing tensile stresses into single point incremental forming to affect martensitic transformation of SS304

To cite this article: E M Mamros et al 2022 IOP Conf. Ser.: Mater. Sci. Eng. 1238 012085

View the article online for updates and enhancements.

You may also like

- <u>Tribocorrosion studies on diamond-like</u> carbon film deposited by PECVD on 304 stainless steel in simulated body fluid S M M Oliveira, I L M Barzotto, L Vieira et al.
- <u>Study on the influence of auxiliary</u> electrode and magnet on electrochemical machining of SS304 using NaCl and NaNO₃
 Deepak J and Hariharan P
- Microstructural, thermo-optical, mechanical and tribological behaviours of vacuum heat treated ultra thin SS304 foils Debajyoti Palai, Manjima Bhattacharya, Amitava Basu Mallick et al.



doi:10.1088/1757-899X/1238/1/012085

Superposing tensile stresses into single point incremental forming to affect martensitic transformation of SS304

E M Mamros¹, F Maaβ², M Hahn², A E Tekkaya², J Ha¹, and B L Kinsey¹

- ¹ Department of Mechanical Engineering, University of New Hampshire, Durham, NH USA
- ² Institute of Forming Technology and Lightweight Components, TU Dortmund University, Dortmund, Germany

elizabeth.mamros@unh.edu

Abstract. Superposing pre-stress on a SS304 sheet metal blank in biaxial tension and performing a single point incremental forming operation on the stretched blank is investigated experimentally. By applying a pre-stress to the sheet metal blank prior to incremental forming, the resulting microstructural change can be affected to obtain functionally graded materials according to the intended application. In austenitic stainless steels, this variation of the stress states alters the phase transformation, specifically the martensitic transformation kinetics, by influencing key process parameters, such as process force, temperature, and equivalent plastic strain. The phase transformation in truncated square pyramids is measured using magnetic induction. These measurements validate the effectiveness of the stress superposition method for achieving the desired mechanical properties based on altering the final microstructure of a simple geometry.

1. Introduction

For rapid-prototyping purposes and applications that require customizable manufacturing, e.g., trauma fixation hardware to hold fractured bones together during healing, which necessitate patient-specific geometries, incremental forming is an excellent candidate among sheet metal forming processes. Incremental forming is a manufacturing process that focuses on localized deformation as one or more tools move across a clamped sheet at varying depths according to the programmed toolpath [1]. This inherent flexibility is essential for low quantity jobs and reducing rapid-prototyping costs. However, incremental forming is not yet commonly used in industry due to existing gaps in knowledge related to how the process parameters affect the final part and the adaptability of the process for specific products.

The most common type of incremental forming is single point incremental forming (SPIF), which uses one tool to deform a clamped blank. This can be performed in a computer numerical control (CNC) milling machine, i.e., it does not require specialized equipment, and is easily integrated into existing manufacturing environments [2]. Alternatively, a robotic arm can be used to perform this process in an industrial setting [3]. For axisymmetric geometries, a SPIF process, commonly referred to as metal spinning, can be used [4]. These processes are suitable for a variety of materials ranging from steels to composites to polymers.

Austenitic stainless steels, which undergo strain-induced transformation into a stronger, more brittle phase, i.e., martensite [5,6], are of interest for many applications, including the automotive, aerospace,

Content from this work may be used under the terms of the Creative Commons Attribution 3.0 licence. Any further distribution of this work must maintain attribution to the author(s) and the title of the work, journal citation and DOI.

doi:10.1088/1757-899X/1238/1/012085

and biomedical industries. Several studies have investigated the extent to which the phase transformation from γ -austenite to α '-martensite can be influenced by adjusting the process parameters e.g., in SPIF [7,8] and deep drawing [9]. This also affects the material formability [10] and residual stress development [11]. Increased phase transformation is desired in areas of the part requiring increased strength, e.g., mounting locations in trauma fixation hardware.

A novel incremental forming process variant introduced in [12] is tensile stress-superposed incremental forming (TSSIF), which uses a custom frame to pre-stress the sheet in-plane to affect the final part properties, e.g., residual stress development. TSSIF is an example of stress superposition, which is generally defined as the incorporation of additional stresses into an existing manufacturing process during a single operation [13,14]. By adjusting the intensity of the stress superposition, i.e., changing the amount of pre-stress imposed on the clamped blank, the final part properties can be tailored for the intended application of the final product.

In this paper, the effect of stress superposition on the phase transformation in SS304 truncated square pyramids formed by SPIF and TSSIF is presented. Force and temperature data are recorded during experiments. After forming, the geometrical accuracy and final strain state are assessed using a photogrammetry camera. Magnetic induction is used to measure the phase transformation from γ -austenite to α '-martensite at four locations on each wall of the formed pyramids. Increased martensite transformation is observed at the base and middle of parts formed by TSSIF, indicating that stress superposition can be used in incremental forming to create functionally graded materials.

2. Incremental Forming Experiments

2.1. Material, Geometry, and Experimental Setup

Experiments are conducted at the Institute of Forming Technology and Lightweight Components (IUL). Blanks for incremental forming, with the geometry shown in Figure 1a, are laser cut from sheets of 0.8 mm thick SS304 (EN 1.4307). A dot pattern with 1 mm diameter dots and 2 mm grid spacing is electrochemically etched onto one side of the blank prior to forming for 3D optical measurements of the formed part. The investigated geometry is a truncated square pyramid with a 45° wall angle (β), 30 mm height (h), and 85 mm base (b) as shown in **Figure 1**b. A 5-axis DMU 50 milling machine (DMG Mori) performs the incremental forming operation by using its computer numerical control to follow the userspecified toolpath. A custom tensile frame with hydraulic cylinders is placed inside of the milling machine to serve as the blank holder during SPIF and the means to induce tensile stress superposition during TSSIF. During SPIF, all four sides of the blank are clamped and fixed in the tensile frame with the cylinders pressurized just enough to prevent displacement. During TSSIF, the blank is fixed on two sides while the remaining two sides are pulled in tension along the positive x- and y-axes by the pressurized cylinders in the frame. In this work, the application of the pre-stress for TSSIF results in an average of 1% von Mises strain in the forming area, which was determined using ARGUS (GOM Inc.). The material's rolling direction (RD) is aligned with the x-axis. The complete experimental setup is shown in Figure 2.

IOP Conf. Series: Materials Science and Engineering

1238 (2022) 012085

doi:10.1088/1757-899X/1238/1/012085

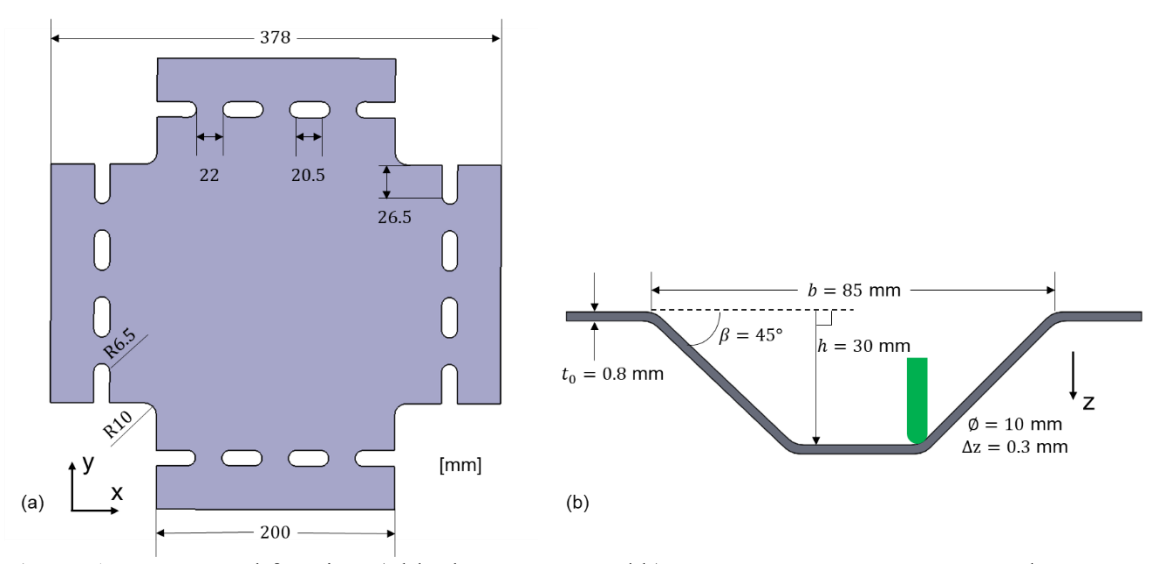


Figure 1. Incremental forming a) blank geometry and b) target part geometry: truncated square pyramid.

For both incremental forming processes, i.e., SPIF and TSSIF, the following parameters are used. The hemispherical tool has a diameter (\emptyset) of 10 mm, and the step down (Δz) is 0.3 mm (Figure 1b). The tool rotational speed is set to 0 rpm, i.e., fixed, and the feed rate is 1500 mm/min. The tool follows a bidirectional toolpath with the start point located in the same corner of the geometry for each layer and forms the pyramid from the base to the top, i.e., outside-in toolpath. The surface of the blank is lubricated with a thin layer of deep-drawing oil (Castrol) prior to forming. The forming process time is approximately 840 s.

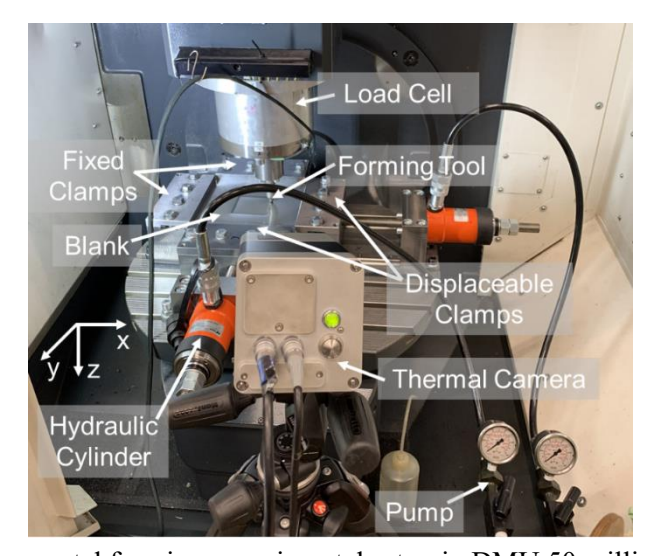


Figure 2. Incremental forming experimental setup in DMU 50 milling machine.

2.2. Data Collection

A three-directional load cell (Kistler) measures the forces from the tool, and a thermal camera (VarioCAM HD head) measures the temperature field during the process. These data are analyzed using Catman Easy (HBM) and IRBIS 3 (InfraTec) software, respectively. The geometrical accuracy of the unclamped part is compared to the computer-aided design (CAD) target geometry using ARGUS. Using

the electrochemically etched dot pattern, the strain state after forming on the non-tool-side is also analysed with ARGUS. An FMP30 Feritscope (Fischer Technology Inc.) is used to determine the α '-martensite volume fraction at four locations along each wall of the truncated square pyramid through magnetic induction with the conversion factor from the ferrite number to the α '-martensite content proposed by Talonen et al. [15]. Feritscope measurements, performed on the tool-side of the workpiece, are repeated three times at each location and then averaged.

3. Results and Discussion

3.1. Force and Temperature Results

In the first half of the forming process (~420 s), the axial force is noticeably higher for TSSIF than SPIF (**Figure 3**a). This is due to the differing stress states of the blank and boundary conditions between the two processes. The biaxial tensile stress superposition in-plane increases the axial, i.e., z- or normal, force initially during TSSIF since the sheet is less susceptible to bending than during SPIF, and the geometry is still relatively planar. However, near the end of the forming process (~>600 s), TSSIF results in axial forces that are approximately equal to those in SPIF.

Correspondingly, the maximum observable temperature in the forming area is higher for TSSIF than SPIF for the entire forming process until the end, where the temperature is similar for the two processes (**Figure 3**b). The insets in **Figure 3**b are thermal images captured approximately when Location 2 was being formed by TSSIF and SPIF. Note that the maximum temperature value in the forming area is located beneath the tool and not visible to the thermal camera, i.e., the total temperature increase is $> 50^{\circ}$ C. The similar temperatures near the end of the forming process, i.e., at the top of the truncated pyramid geometry, can be attributed to similar axial forces, heat dissipation, and plastic strain in this location for SPIF and TSSIF. Note that the four approximate locations for strain and α '-martensite measurements are indicated in Figure 3.

From **Figure 3**, the superposed stress is effective as long as the part is still nearly planer (up to ~ 500 s and including Locations 1 and 2). For the remainder of the TSSIF forming process, the effect of the planar superposed stress diminishes. This explains the similar axial force and temperature levels for SPIF and TSSIF near the end of the forming processes.

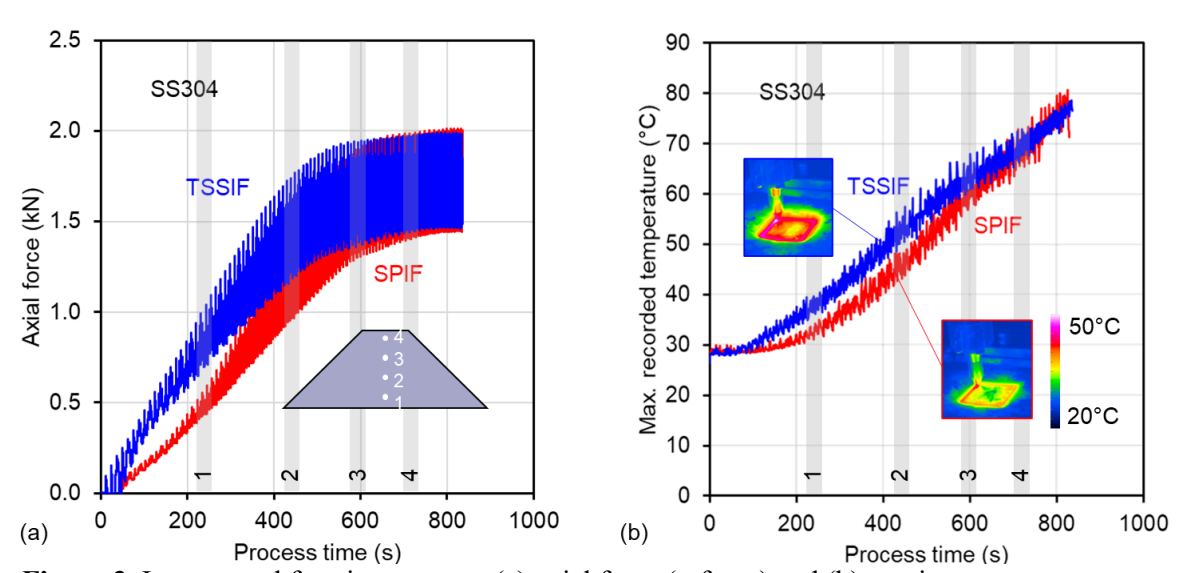


Figure 3. Incremental forming process: (a) axial force (z-force) and (b) maximum temperature recorded by thermal camera and thermal images captured at Location 2.

doi:10.1088/1757-899X/1238/1/012085

3.2. Geometry Comparison

Springback, resulting from the elastic recovery of the material, occurs when the formed part is removed from the clamping mechanisms [16]. In the case of TSSIF, springback also occurs in-plane when the pressure is released from the cylinders in the frame. To compare the geometrical accuracy of the SPIF and TSSIF processes, a 100 mm subsection of the formed parts, which includes the truncated square pyramid geometry and ~7.5 mm of the flange, is considered. A section cut is made along the x- and y-axes through the geometrical center of the truncated square pyramid (see inset figure in **Figure 4**). The resulting profiles for SPIF, TSSIF, and the target geometry along the x-direction (solid) and y-direction (dashed) are shown in **Figure 4**.

For SPIF and TSSIF, the profiles along the x- and y- directions are nearly symmetrical, and the deviation from the target heights are \sim 7 and 5.6 mm, respectively, at the corner near the base of the truncated pyramid. For TSSIF, all four sides of the truncated pyramid formed by TSSIF have increased geometrical accuracy in the z-direction near the base of the truncated pyramid compared to SPIF. When comparing the wall angles in the formed parts, the TSSIF profiles tend to follow the target profile more closely than SPIF. Overall, the truncated square pyramid manufactured by TSSIF achieves greater geometrical accuracy than the part manufactured by SPIF with respect to the target geometry.

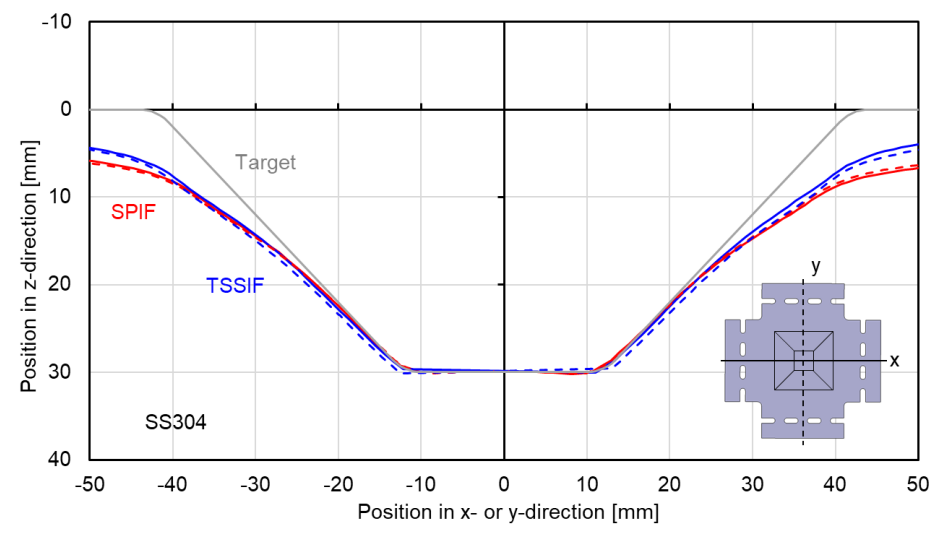


Figure 4. Profiles along the center of truncated square pyramids in the x- (solid) and y- (dashed) directions for target geometry and parts manufactured by SPIF and TSSIF.

3.3. Final Strain State

To compare the final strain state of the parts manufactured by TSSIF and SPIF after removal from the frame, a 90x90 mm² section is analyzed. The von Mises strain contours are shown in **Figure 5**. The white circles represent the four measurement locations along the pyramid walls (see inset figure in **Figure 5**b) plotted in **Figure 6**a. The von Mises strain near the outer edges of the analyzed area, i.e., at the base, and at the top of the truncated pyramid is nearly zero as expected due to minimal deformation in these areas of the geometry. In TSSIF, a larger uniform strain region is visible on the truncated pyramid walls compared to SPIF. For both forming processes, the maximum strain is located along the diagonals, where the tool changes directions, with a slightly increased strain along the top right diagonal, which corresponds to the starting point for each layer of the toolpath.

In Figure 6a, discrete von Mises strain values are shown for SPIF (squares) and TSSIF (triangles) at the four locations, i.e., 1-4, for all four faces of the truncated square pyramid geometry (see inset figure in **Figure 6**a for color map) on the non-tool-side. As is similarly presented in **Figure 5**, TSSIF produces

a larger plastically deformed area along the wall (see the orange to red zone in Figure 5), with higher von Mises strain values near the base and middle of the truncated square pyramid, i.e., Locations 1-3 in Figure 6a. This leads to reduced springback when the stress superposition is imposed in the experiments as is shown in Figure 4.

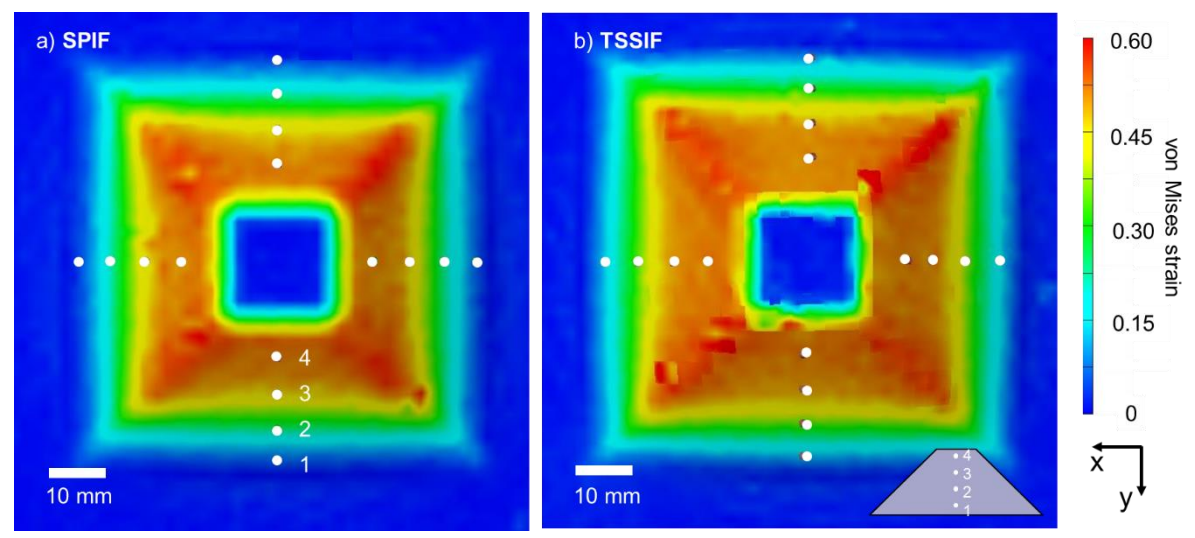


Figure 5. Final strain state of unclamped parts manufactured by a) SPIF and b) TSSIF. Circles represent Locations 1 – 4 on pyramid wall.

3.4. Phase Transformation

The as-received sheet material is fully austenitic and is subjected to strain-induced transformation into α'-martensite as a result of incremental forming. In Figure 6b, the α'-martensite volume fraction is shown for SPIF (squares) and TSSIF (triangles) at the four locations on the tool-side of the truncated square pyramid geometry. The average of the four sides for each location is also included as solid (TSSIF) and dashed (SPIF) lines to indicate the phase transformation trends in Figure 6b. Near the base at Locations 1 and 2, the largest differences of α '-martensite volume fraction are observed between TSSIF and SPIF, i.e., 0.051 and 0.049, respectively. Assuming that the average von Mises strain of ~0.01 in the forming area after pre-stressing the blank is negligible, this indicates that the effect of the tensile stress superposition on the phase transformation is strongest in the first few layers of the toolpath. The increased axial force at these locations in Figure 3a is due in part to the presence of the stronger α'-martensite material phase. In the middle at Location 3, TSSIF still experiences greater phase transformation than SPIF, i.e., 0.012, and the largest phase transformation overall for the four locations measured in the TSSIF part. At the top of the geometry, i.e., Location 4, the effect of the tensile stress superposition is no longer apparent, and other parameters affecting the phase transformation, e.g., temperature, may become dominant since the strain levels at Locations 3 and 4 are comparable for TSSIF (Figure 6a). The decrease in volume percent of α '-martensite observed for TSSIF when comparing Locations 3 and 4 may be caused by the increased temperature in the forming area (see Figure 3b), which is known to inhibit austenite to martensite phase transformation [8,17]. Note that correction factors based on the material thickness are provided by the manufacturer (but not included in these results) and may result in martensitic volume fractions up to 1.15 times those reported in this work [18].

doi:10.1088/1757-899X/1238/1/012085

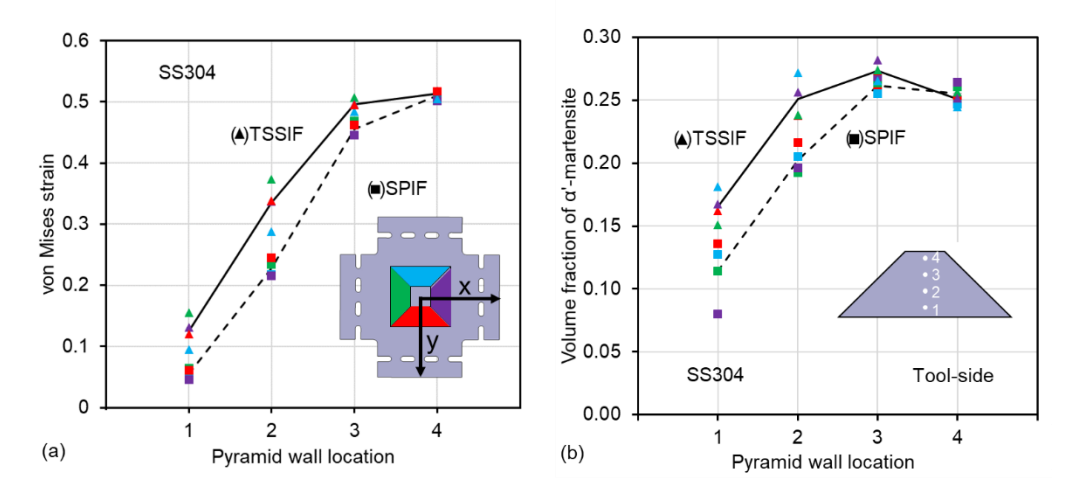


Figure 6. Truncated square pyramid parts manufactured by TSSIF (triangles) and SPIF (squares): (a) von Mises Strain and (b) volume fraction of α '-martensite measured on tool-side. Average values shown as solid (TSSIF) and dashed (SPIF) lines.

4. Conclusions and Future Work

In this paper, biaxial tensile stress is superposed into the single point incremental forming process, i.e., TSSIF, to affect the martensitic transformation of SS304 for a truncated square pyramid geometry. Initially, increased and then, ultimately, similar axial forces and temperatures are observed for TSSIF when compared to the conventional process, i.e., SPIF. The overall geometrical accuracy of the part manufactured by TSSIF is greater than that of the part manufactured by SPIF, particularly for the part height. The stress superposition in TSSIF aids the reduction of the springback in the final part. A larger uniform strain area along the pyramid walls and increased phase transformation is observed at Locations 1, 2, and 3 of the pyramids manufactured by TSSIF compared to SPIF. Therefore, the methodology of using stress superposition in incremental forming is successful in influencing the phase transformation and altering the microstructure in the final part.

Several parameters, e.g., temperature and stress and strain states, contribute to the phase transformations in this austenitic stainless steel. Additional modelling efforts are needed to better understand which effects are dominating at varying points throughout the toolpath. Future work will aim to establish a fundamental understanding of this phenomenon and to more effectively influence the transformation kinetics with the stress superposition effect, e.g., through higher pre-stress or lowering the temperature in the process. An additional material characterization method, e.g., electron backscatter diffraction, will be used to validate the martensite volume fractions.

5. Acknowledgements

Support for the New Hampshire Center for Multiscale Modeling and Manufacturing of Biomaterials (NH BioMade) project is provided by the US National Science Foundation (NSF) EPSCoR award (#1757371). This research is also supported by the Institute of International Education Graduate International Research Experiences program (NSF #1829436), the German-American Fulbright Commission, and the Germanistic Society of America.

doi:10.1088/1757-899X/1238/1/012085

References

- [1] Cao, J., Huang, Y., Reddy, N. V., Malhotra, R., and Wang, Y., 2008, "Incremental Sheet Metal Forming: Advances and Challenges," pp. 1967–1982.
- [2] Martins, P. A. F., Bay, N., Skjoedt, M., and Silva, M. B., 2008, "Theory of Single Point Incremental Forming," CIRP Ann., 57(1), pp. 247–252.
- [3] Schafer, T., and Dieter Schraft, R., 2005, "Incremental Sheet Metal Forming by Industrial Robots," Rapid Prototyp. J., 11(5), pp. 278–286.
- [4] Rentsch, B., Manopulo, N., and Hora, P., 2017, "Numerical Modelling, Validation and Analysis of Multi-Pass Sheet Metal Spinning Processes," Int. J. Mater. Form., **10**(4), pp. 641–651.
- [5] Feng, Z., Mamros, E. M., Ha, J., Kinsey, B. L., and Knezevic, M., 2021, "Modeling of Plasticity-Induced Martensitic Transformation to Achieve Hierarchical, Heterogeneous, and Tailored Microstructures in Stainless Steels," CIRP J. Manuf. Sci. Technol., 33, pp. 389–397.
- [6] Mamros, E. M., Bram Kuijer, M., Davarpanah, M. A., Baker, I., and Kinsey, B. L., 2021, "The Effect of Temperature on the Strain-Induced Austenite to Martensite Transformation in SS 316L During Uniaxial Tension," *Forming the Future*, G. Daehn, J. Cao, B. Kinsey, E. Tekkaya, A. Vivek, and Y. Yoshida, eds., Springer International Publishing, Cham, pp. 1853–1862.
- [7] Katajarinne, T., and Kivivuori, S., 2013, "Strain Induced Martensite in Incremental Forming Formation, Effect and Control," Mater. Sci. Forum, 773–774, pp. 119–129.
- [8] Katajarinne, T., Louhenkilpi, S., and Kivivuori, S., 2014, "A Novel Approach to Control the Properties of Austenitic Stainless Steels in Incremental Forming," Materials Science and Engineering: A, **604**, pp. 23–26.
- [9] Krauer, J., and Hora, P., 2012, "Enhanced Material Models for the Process Design of the Temperature Dependent Forming Behavior of Metastable Steels," Int. J. Mater. Form., 5(4), pp. 361–370.
- [10] Lonardelli, I., Bosetti, P., Bruschi, S., and Molinari, A., 2011, "On the Formability and Microstructural Characteristics of AISI 301 Parts Formed by Single-Point Incremental Forming," Key Eng. Mater., 473, pp. 869–874.
- [11] Afzal, M. J., Maqbool, F., Hajavifard, R., Buhl, J., Walther, F., and Bambach, M., 2020, "Modeling the Residual Stresses Induced in the Metastable Austenitic Stainless Steel Disc Springs Manufactured by Incremental Sheet Forming by a Combined Hardening Model with Phase Transformation," Procedia Manuf., 47, pp. 1410–1415.
- [12] Maaß, F., Hahn, M., and Tekkaya, A. E., 2022, "Setting Residual Stresses in Tensile Stress-Superposed Incremental Sheet Forming," *Proceedings of the 22nd International Conference on Material Forming*.
- [13] Mamros, E., Ha, J., Korkolis, Y., and Kinsey, B., 2020, "Experimental Investigation and Plasticity Modeling of SS316L Microtubes Under Varying Deformation Paths," J. Micro Nano-Manuf.
- [14] Maaß, F., Hahn, M., and Tekkaya, A. E., 2021, "Adjusting Residual Stresses by Flexible Stress Superposition in Incremental Sheet Metal Forming," Arch. Appl. Mech., 91(8), pp. 3489–3499.
- [15] Talonen, J., Aspegren, P., and Hänninen, H., 2004, "Comparison of Different Methods for Measuring Strain Induced Martensite Content in Austenitic Steels," Mater. Sci. Technol., 20, pp. 1506–1512.
- [16] Hosford, W. F., and Caddell, R. M., 2011, *Metal Forming: Mechanics and Metallurgy*, Cambridge University Press.
- [17] Olson, G., and Cohen, M., 1975, "Kinetics of Strain-Induced Martensitic Nucleation," Met. Trans A, 6, pp. 791–795.
- [18] Helmut Fischer GmbH, 2008, "Operators Manual Feritscope FMP30."